coatings

MDPI

Article

Particle Compression Test: A Key Step towards Tailoring of Feedstock Powder for Cold Spraying

Hamid Assadi [1,*] and Frank Gärtner [2]

[1] Brunel Centre for Advanced Solidification Technology, Brunel University London, Uxbridge UB8 1XU, UK
[2] Institute of Materials Technology, Helmut Schmidt University, 22043 Hamburg, Germany; Frank.Gaertner@hsu-hh.de
* Correspondence: hamid.assadi@brunel.ac.uk

Received: 15 April 2020; Accepted: 6 May 2020; Published: 9 May 2020

Abstract: Cold spray is on the way to becoming a mainstream technology for coating and additive manufacturing processes. While there have been many advances in various aspects of this technology, the question of tailoring the 'ideal' feedstock powder for cold spraying has remained open. In particular, the mechanical strength and its dependence on the particle size, which are amongst the most relevant properties of the feedstock powder for cold spraying, are rarely covered when reporting powder specifications. This is mainly because of the lack of standardised methods of characterisation for these specific properties. In the present case study, we demonstrate how compression tests of single Inconel 718 particles by using a modified nanoindenter can address this central question. Data analyses are supported by finite element modelling of particle compression for a range of plastic behaviours. The results of simulation are then stored in the form of a surrogate model for subsequent comparison with the experimental data. Thus, the ultimate tensile strength and the size of the examined particles are calculated directly from the measured force-displacement data. The paper will also discuss how this information can be used to optimise cold spraying, and so, unveils a key step towards the design and manufacturing of cold-spray-specific feedstock powder.

Keywords: cold spray; powder; characterisation; mechanical properties; particle compression

1. Introduction

There is a growing interest in cold spraying as a coating method due to its unique characteristics [1–3]. The solid-state nature of the process, in combination with a relatively high deposition rate, makes it a particularly attractive technology for additive manufacturing (AM) and repair. This has thrusted many research, development, and commercial activities on various aspects of cold spray technology, from experimenting with new materials and new applications to nozzle design and equipment manufacturing.

However, a major remaining hurdle in the way of widespread application of cold spray is the lack of tailored and standardised feedstock powder. This has forced researchers and users to experiment with what is in fact tailored and made commercially available for other processes, such as conventional powder metallurgy (PM), thermal spraying or laser-based AM. The available powders in the market do not appear to be accompanied with any cold-spray-specific technical data, albeit being branded as cold spray powder.

There is a fundamental problem with the above approach to powder selection. In conventional thermal spraying, PM as well as AM, the prime properties of the feedstock powder are the chemical composition and particle size distribution. There is rarely any information available on the mechanical strength of the particles of the powder, simply because it is not a relevant property where the material is to melt and to re-solidify during the process. In cold spraying, in contrast, the mechanical properties,

namely the plastic behaviour and the ultimate tensile strength (UTS) of single particles, are the most important characteristics that determine whether the process will work and if so, what will the quality of the deposited material be like.

As a workaround to this problem, plastic properties of microparticles are often inferred from the available bulk data. However, particles are likely to exhibit different properties from the bulk material. This is because of the possible differences in microstructure, due to different processing conditions during production, in level of impurities, and in oxygen content. Moreover, bulk data may not exist for some alloys, which are produced only in powder form.

Local methods such as hardness testing on the cross section of particles do not provide a solution to this problem. This is partly because of using a mounting material, which deforms under loading and hence interferes with the results of measurements. In addition, these locally applied methods would not provide information on the global deformation behaviour of particles, which is relevant for cold spray applications. This is because the particles also deform globally during cold spraying, hence taking in the collective effect of microstructural inhomogeneities rather than their local mechanical response.

There have been efforts to determine the mechanical properties of particles, mainly for PM applications [4], but only for specific plastic behaviours. In a previous work [5], we developed a method to work out plastic constitutive properties of the particles for a wide range of possible behaviours, through a combination of modelling and compression tests using a modified nanoindenter. The method was used to determine plastic constitutive properties of copper and MCrAlY particles of known dimensions. In a recent report on cold spraying of Inconel 718, it could be shown that particle strength of as-atomized powder is about 20% higher than that of soft annealed bulk material, thus using the real strength data will allow for a much more reliable prediction and interpretation of coating performance [6]. In the present work, we extend the method to determine not only the plastic behaviour but also the size of the particles of an Inconel 718 powder. We demonstrate that the extended method, in which the particle size is taken as an 'unknown' adjustable parameter, provides a better fit between the modelling and the experimental data, and so, allows a more reliable estimation of the relationship between the strength and the particle size. Based on these results, the paper discusses the implication of the method for cold spray applications, and in the prediction of coating quality.

2. Methods

Step 1: Initially, the finite element analysis (FEA) software package ABAQUS version 6.12 was employed to simulate the non-linear deformation of particles during the compression tests. The simulations were performed using an axisymmetric model of a 50 μm deformable sphere (particle), with a mean element size of 0.5 μm, squeezed between two rigid plates approaching one another at a constant displacement rate. The calculation domain included only half of the sphere, with z-symmetry applied to the bottom boundary. An explicit Lagrangian method with mass-scaling was used for the simulations, which were performed for a range of constitutive properties. A typic friction coefficient of 0.5 was used for the interaction between the particle and the rigid plates (for more details of the non-linear finite element analysis employed in this study see [5]). The flow stress of material (σ) was described as a function of the plastic strain (ε) according to the following relationship:

$$\sigma = A + B\varepsilon^n \tag{1}$$

in which A, B and n are constants. The force-displacement (F–δ) relations as obtained from the simulations were subsequently converted to nominal stress–strain relations as a function of particle dimensions as follows:

$$\sigma_{nom} = \frac{4F(d_0 - \delta)}{\pi {d_0}^3},\ \varepsilon_{nom} = -ln\left(1 - \frac{\delta}{d_0}\right) \tag{2}$$

where d_0 is the mean particle diameter, which is identical to its height (h_0) for a perfectly spherical particle. The simulated results supply the stress–strain relations for the given set of material parameters for subsequent comparison with the experimental data at a later step.

Step 2: Compression tests of 16 single particles of a gas atomised Inconel 718 powder with the nominal size of 10–28 μm, branded as Ni 202 from Praxair Surface Technologies (Indianapolis, IN, USA) were carried out (by careful handling and positioning of individual particles) under quasi-static conditions using a universal hardness testing machine (model ZHU 2.5/Z2.5 from Zwick GmbH & Co. KG, Ulm, Germany) with a flat diamond head of 200 μm diameter. The examined particles had a predominantly dendritic microstructure and spheroid geometry (Figure 1), with an average diameter between 10 and 25 μm. They were placed individually on the surface of a mirror polished hard substrate (WC-Co composite, hardness: 1780 HV2) and compressed with a constantly increasing displacement, at a speed of 0.1 mm/min, up to a maximum load of 1.2 N. The size of the particles was measured before deformation using confocal microscopy (3D Laser Scanning Microscope VK-X200 series from KEYENCE GmbH, Neu Isenburg, Germany) for comparison with the calculated size. The confocal microscopy can provide highly precise measurements (100 nm range) of the dimensions of an object. However, the particles are not ideally spherical (Figure 1) so that the measured dimensions (d_0 and h_0) are only representative of the nominal particle size, hence they do not necessarily correspond to the respective values under the compression testing. This is so simply because the particles are likely to have different orientations during the confocal microscopy measurements and the compression tests. Therefore, while the measurements have a 100 nm precision, their accuracy is limited by the ovality of the particles (the difference between the largest and the smallest dimensions), which can be in the range of up to a few (2–3) μm. Table 1 shows the measured dimensions for a selection of particles. Figure 2 shows examples of images of the particles before and after deformation as obtained by confocal microscopy. The micrographs of the compressed particles indicate that, despite the rather spherical shape before testing, deformation can cause shape irregularities. This is probably due to differences in orientation, hence plasticity of the grains of the particle. After the compression tests, the measured force-displacement data were translated into nominal stress and strain values using Equation (2).

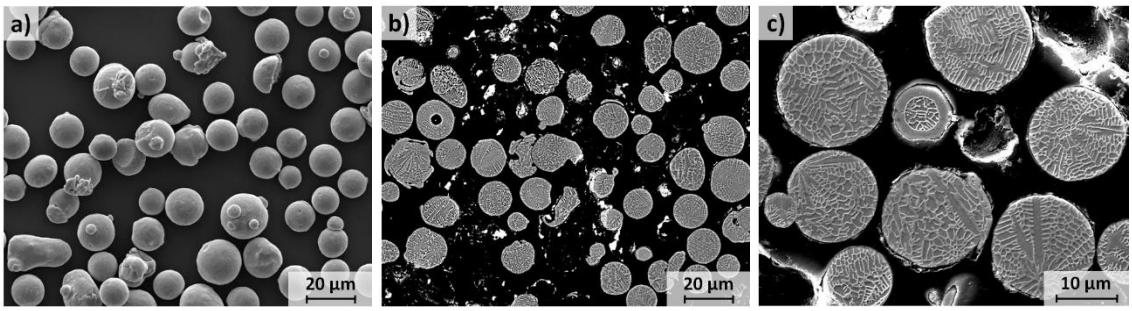

Figure 1. SEM micrographs showing (**a**) the morphology and (**b**,**c**) the cross-section of the particles of the examined Inconel 718 powder.

Table 1. Measured particle dimensions.

Particle Number	1	2	3	4	5	6	7
d_0 (m)	19.7	19.7	16.7	20.7	18.9	16.0	15.0
h_0 (m)	20.4	21.0	17.7	20.2	16.6	15.0	13.0

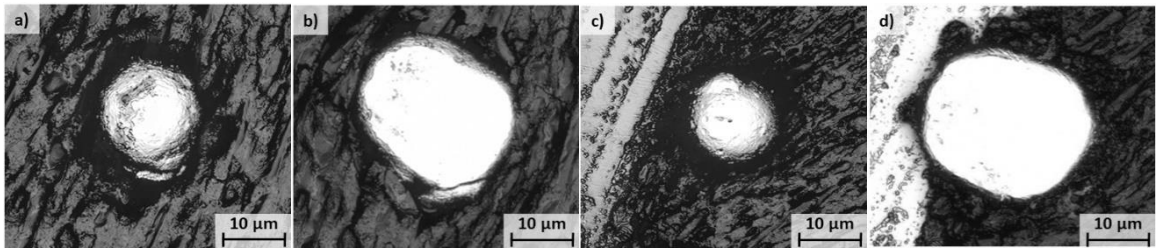

Figure 2. Examples of confocal microscopy images of the particles: (**a**,**b**) particle #5, (**c**,**d**) particle #3 (dimensions given in Table 1) before (**a**,**c**) and after (**b**,**d**) deformation, respectively.

Step 3: The experimental data for 7 (out of the 16 tested) particles were assessed against the modelling results as obtained in step 1. The constitutive parameters A, B and n, as well as the particle size, d_0, varied within a range until the best fit was obtained between the modelled and experimental data. The final values of A, B, n and d_0 were taken as representing the relevant plastic constitutive properties and the size of the examined particle. Once these parameters were known, then the ultimate tensile strength (UTS) was calculated using the relation: $\sigma = d\sigma/d\varepsilon$.

The fitting procedure was performed using an in-house program that directly operates on the uploaded raw data generated by the instrument. The program uses a least squares method where the experimental and modelled nominal data were compared for 19 equidistant points along the nominal strain axis, giving the best-fit parameters along with a fitting quality (Q) defined as follows:

$$Q = 100\left(1 - \frac{\overline{\left|\sigma_{\text{experiment}} - \sigma_{\text{model}}\right|}}{UTS}\right) \tag{3}$$

Figure 3 shows a schematic of the above procedure to work out the constitutive properties and size of the particles. To illustrate the relevance of this procedure for cold spray application, the corresponding 'quality parameter' $\eta = v_p/v_{cr}$ (with v_p as the particle impact velocity and v_{cr} as the critical velocity at the particle impact temperature) for different scenarios was calculated based on the equations given by Assadi et al. [7], using a web-based program provided by Kinetic Spray Solutions GmbH, Buchholz, Germany [8] for a typical set of spraying parameters for Inconel 718. For these calculations to be in general consistent with the real experiments performed by using the nozzle type 'D24' from CGT (Ampfing, Germany) equivalent to 'Out1' from Impact Innovations (Haun/Rattenkirchen, Germany) [6,9], the spray conditions were assumed as follows: p_{gas} = 50 bar, T_{gas} = 1000 °C, powder injection at 135 mm upstream of the nozzle throat, and a powder injection stream speed of 5 m/s. The carrier gas flow rate and the standoff distance are set to 5% of the total flow rate and 20 mm, respectively.

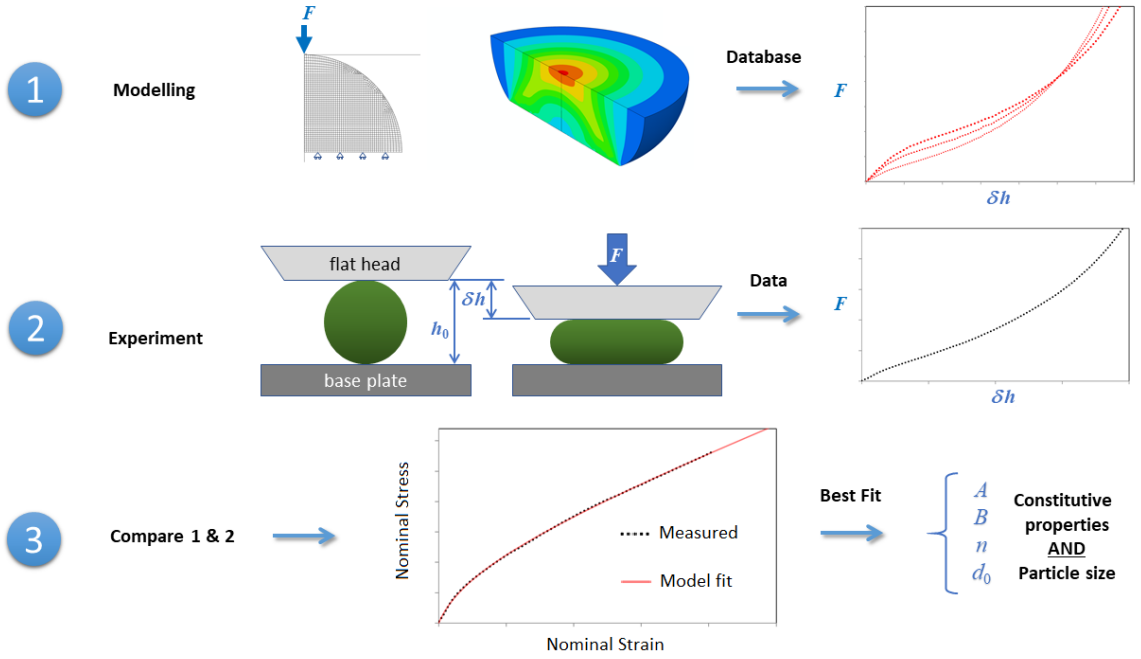

Figure 3. Flow chart of the method used to determine the constitutive properties and the size of the particles of cold-spray powders by modelling (**1**), experiments (**2**), and fitting (**3**).

3. Results

Figure 4 shows a representative selection of the results as obtained from the compression tests for Inconel 718 particles, indicating a similar force-displacement trend. These data are converted to nominal stress–strain relationships using Equation (2) and then fitted with modelled relationships for two cases as follows: (a) the particle dimensions are fixed and set to the measured values, and (b) the particle size is taken as an adjustable parameter. The results of these two fitting procedures are shown in Figures 5 and 6. For both procedures, a very good match could be obtained between the modelled and the experimental data for the respective set of fitting parameters (Table 2). However, the match appears to improve for particle #3 when the particle size is treated as an adjustable fitting parameter. For this particle, the predicted size shows a higher deviation to the measured value as compared to the other ones of this selection.

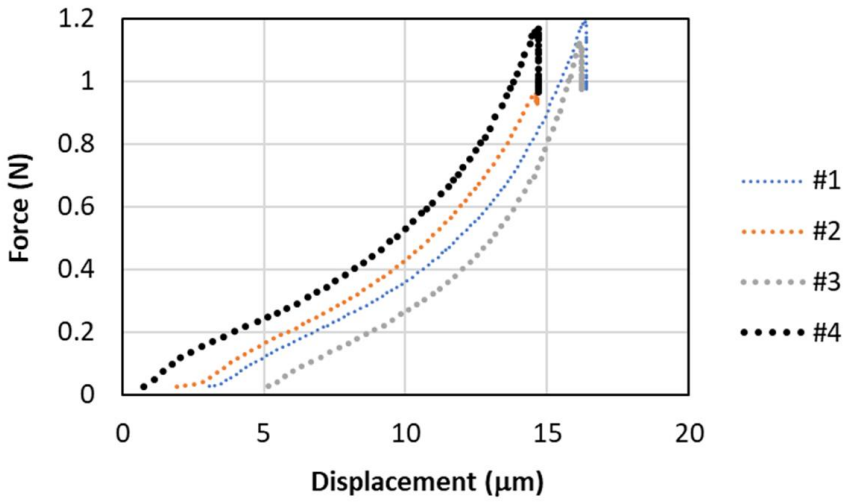

Figure 4. Selected results of raw force-displacement data from compression experiments for Inconel 718 particles of different dimensions (Table 1, particles #1–4) as measured by confocal microscopy.

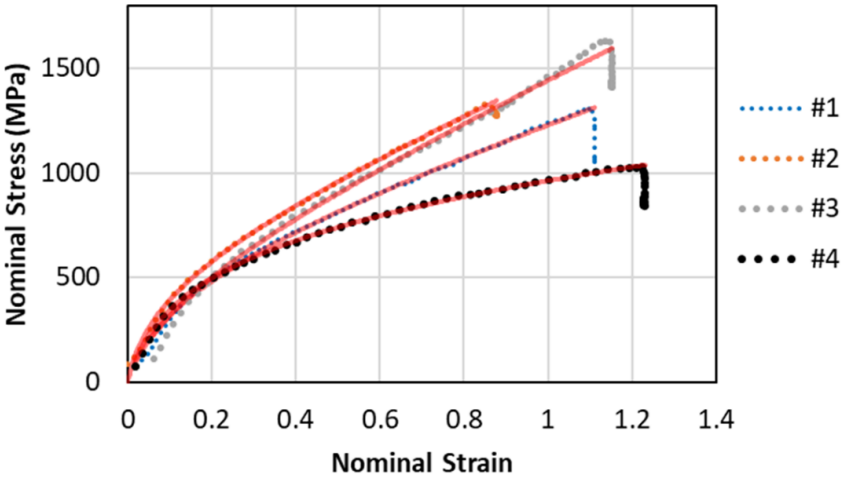

Figure 5. Selected results of the first fitting procedure, where the particle dimensions are fixed and set to the measured values, as applied to the compression test data (converted to nominal stress–strain) for Inconel 718 particles #1–4 (Table 1). The dotted lines are the converted measured data and the solid lines (50% transparent, red in the colour version) are the fitting curves.

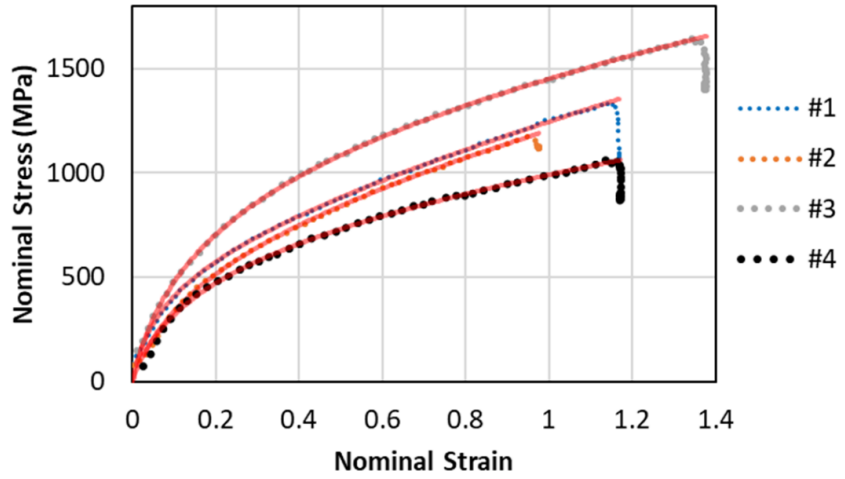

Figure 6. Selected results of the second fitting procedure, the particle size is taken as an adjustable fitting parameter, as applied to the same compression test data as shown in Figure 5, for Inconel 718 particles #1–4 (Table 1). The dotted lines are the converted measured data and the solid lines (50% transparent, red in the colour version) are the fitting curves.

Table 2. Examples of fitting parameters and the estimated ultimate tensile strength (UTS) for particles #1–4, as obtained from the two different fitting procedures.

Method	Quantity	Symbol (Unit)	Particle Number 1	2	3	4
Measurement	Diameter	d_0 (μm)	19.7	19.7	16.7	20.7
Least-squares fitting, fixed particle size	Fitting parameter 1	A (MPa)	655	860	515	500
	Fitting parameter 2	B (MPa)	1580	1720	1990	1060
	Fitting parameter 3	n	0.65	0.70	0.65	0.30
	Ultimate tensile strength	UTS (MPa)	1483	1688	1716	1123
	Fit quality	%	99.3	99.7	98.2	99.5
Least-squares fitting, adjustable particle size	Fitting parameter 1	A (MPa)	1070	850	650	950
	Fitting parameter 2	B (MPa)	1140	1420	1730	860
	Fitting parameter 3	n	0.70	0.70	0.35	0.65
	Fitting parameter 4	d (μm)	18.7	20.4	15.2	20.6
	Ultimate tensile strength	UTS (MPa)	1386	1447	1668	1178
	Fit quality	%	99.7	99.8	99.7	99.6

Figure 7 shows the results of particle size evaluation from the compression test data as compared with the measured values. As shown in Figure 7a, the calculated values correlate well with the measurements, although the calculated particle sizes are slightly below the measured values, particularly for the smaller particles. As displayed in Figure 7b, nevertheless, the overall quality of displacement data fitting in all cases improves when the particle size is relaxed and taken as an adjustable parameter.

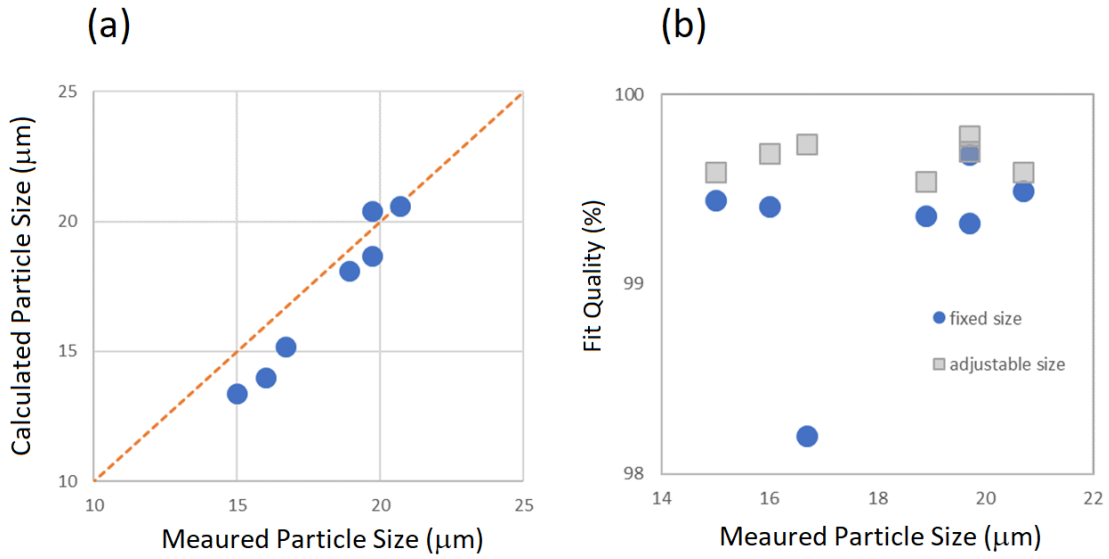

Figure 7. Comparison of the results of particle size determination through direct measurements by confocal microscopy and evaluation by fitting the compression test data: (**a**) showing a comparison between the calculated and the measured values, and (**b**) the fitting quality for the two procedures (Figures 5 and 6).

Figure 8 shows the results of calculated UTS for all the examined particles, for the two different procedures of assuming fixed and relaxed particle sizes in the fitting procedures. For the former one, the UTS varied between 1100 and 1700 MPa, with a mean value of about 1400 MPa, giving no evidence of particle-size dependence. In the latter one, in contrast, there was an indication of decreasing UTS with increasing particle size.

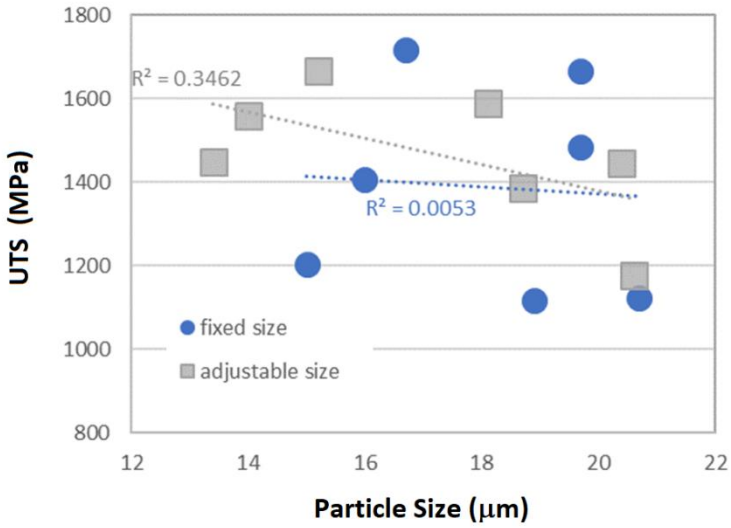

Figure 8. Calculated UTS values of the examined Inconel 718 particles as a function of particle size, for using two different procedures where fitting was performed with and without taking the size as an adjustable fitting parameter.

4. Discussion

The results clearly show that the particle compression tests combined with numerical modelling can be used to determine not only the constitutive plastic properties of metallic particles but also the size of the examined particle. The results of the fitting quality suggest that determination of the particle size based on the force-displacement data might be even more reliable than direct measurements. This has several important implications: (i) reaching a better prognosis for cold spray applications, (ii) allowing to derive size-dependant differences in microstructural developments by solidification, and (iii) advancing mechanical testing procedures in general. These points are discussed below.

For cold spray application, the UTS of the particles of the feedstock powder is the most relevant property of the powder. However, particularly for nickel superalloys, mechanical properties strongly depend on the thermal history of the material. For example, solution-treated and precipitation-hardened Inconel 718 alloys have a UTS of about 900 and 1400 MPa, respectively [10]. In addition, the precipitation-hardened alloy retains a rather high strength of about 1200 MPa up to temperatures of about 600 °C [11]. Thus, the literature data on the bulk material may not be useful for estimating the performance of the feedstock powder in cold spraying. In the case of Inconel 718, for instance, using the data of the soft annealed condition [9] could underestimate UTS, as it would disregard possible influences of rapid solidification on the microstructure. This can lead to substantially overestimated deposition efficiency (DE) and coating quality. Using data for precipitation hardened alloys [10], on the other hand, leads to better estimations of the coating quality (i.e., more consistent with the experimental observations) but it would still be an overestimation. This is because of the anomalous (highly non-linear) thermal softening behaviour of the hardened alloys (retaining their strength up to 600 °C due to the presence of intermetallic phases).

The important role of the particle strength in cold spraying and the above problems in using the existing literature data call for reliable and direct measurement of the particle properties. The method proposed in this paper is a first step in this direction. A second step would be to perform the compression tests at elevated temperature to account for the softening behaviour of the particle, which could differ from that of the bulk. The following is an example of the first step, where the results of the compression tests are used to predict the quality parameter for both methods of data analysis.

Figure 9 shows the influence of the possible size-dependence of the UTS (of the Inconel 718 powder) on the cold-spray velocity ratio, η [3]. For a fixed value of UTS (assumed to be independent of particle size) of 1400 MPa, typical spraying conditions (p_{gas} = 50 bar and T_{gas} = 1000 °C) result in η values ranging from 1.07 to 1.10. By taking the lower bound of the UTS from the literature (i.e., 900 MPa), η increases substantially and varies in the range between 1.28 and 1.31 for the same spraying conditions. In contrast, by using the size-dependent UTS as obtained from the adjustable-size fitting in this study (Figure 8), η falls to a lower range and varies between 1.02 and 1.12. Note that this type of size dependence, as observed for the examined particles in this study, is in addition to (and fundamentally different from) the intrinsic effect of size on the critical velocity due to higher adiabaticity of larger particles [7]. The former effect routes from differences in solidification and thermal history of the particles during powder production, while the effect would be present even if the particles have identical microstructures and differ only in size.

The above differences in η can translate into significant differences in the DE and properties of cold-sprayed deposits. Based on the estimated values of η in this work (which is barely above 1), reaching bulk-like properties by cold spraying with nitrogen, even at high parameter sets, is probably not achievable. A further rise in pressure or temperature to secure the needed velocity ratio of $\eta \gtrsim 1.5$ is not attainable with the state-of-the-art spray equipment. Thus, in most cases, post spray heat treatments are used [6,12,13].

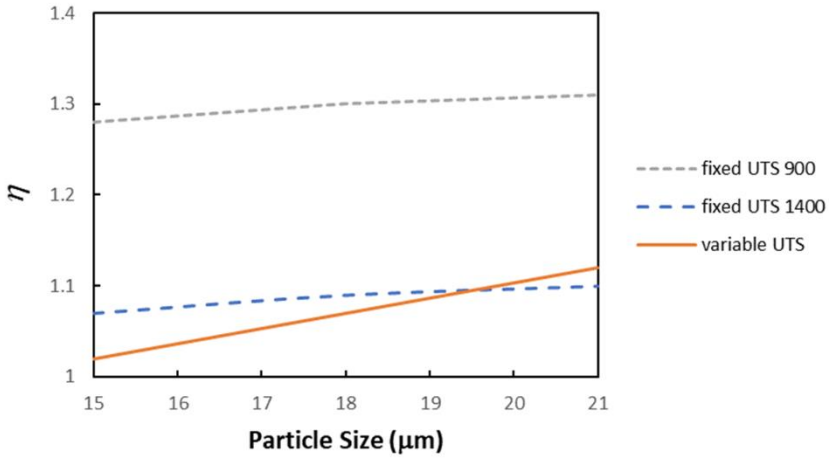

Figure 9. Calculated variation of the velocity ratio $\eta = v_p/v_{cr}$ with particle size for the two cases where the (room-temperature) UTS is fixed and set to 900 and/or 1400 MPa, and where it is assumed to change with particle size (according the variation shown in Figure 8 for the case of adjustable particle size). The ratios are calculated by assuming a cold spray parameter set of p_{gas} = 50 bar and T_{gas} = 1000 °C.

The origin of the size effect as observed in this study is possibly due to differences in the thermal history of the particles during the powder manufacturing (i.e., higher cooling rates in smaller particles) and hence related to differences in solidification microstructure. The range of ultimate tensile strength as evaluated for the examined particles in this work (1200 to 1700 MPa) is already much higher than expected for non-precipitation hardened Inconel 718. The measurements also indicate an increase in the strength with decreasing particles size, which can be attributed to higher undercoolings and cooling rates associated with the solidification of smaller particles. Higher undercoolings/cooling rates can result in the emergence of kinetic effects during rapid solidification, such as solute trapping and non-equilibrium partitioning [14], or dendrite breakup and grain refinement [15], which affect the microstructure and hence properties of the solidified particles. There is also a possibility of chemical influences, namely because of a difference in the level of oxygen. Small particles might have higher oxygen content as compared to larger particles [16]. This difference can also be attributed to the content of flaws and defects in the microstructure of particles, which would be conceivably lower in smaller particles, or to the differences in strain gradient, which would be more prominent in smaller particles. It is unlikely that the differences in strain are due to the so-called dislocation starvation [17,18] which would be expected to become prominent for sub-micron particles, although it cannot be ruled out. Overall, the observed difference in the UTS of the examined particles could be attributed to any of these factors, verification of which will require further studies. The main point here is that the proposed method of analysis—where the particle size is taken as a fitting parameter—implies a size dependence, and that the observed size dependence can have an important influence on cold spray optimisation.

For mechanical testing in general, the current study provides a unique example of a method where mechanical testing is used to work out a dimensional property along with mechanical properties. The current methodology can therefore be extended to other types of mechanical testing to provide fast and accurate dimensional information on embedded defects and microstructural inhomogeneities. The proposed method can therefore be of a broad interest in materials characterisation and hence open a unique opportunity for new research for micro-deformation. Specifically, using spherical samples (instead of micro or nano pillars) can provide more relevant and direct information on powder properties (e.g., for applications in cold spraying or powder metallurgy).

5. Conclusions

Particle compression tests using a modified nanoindenter were combined with FEM simulations to work out the flow-stress of an Inconel 718 powder. The UTS of the examined particles were in the

range 1.1–1.7 GPa. The results also suggest that the UTS is a function of particle size (i.e., UTS increases with decreasing particle size). However, the correlation between the UTS and particle size becomes evident only when the particle size is taken as an adjustable fitting parameter. The particle diameters obtained in this way are slightly different from the measured values. Interestingly, the fitting quality improves when the particle size is taken as an adjustable parameter during fitting. This suggests that the particle size estimated in this way is probably even more accurate and relevant than the values obtained from confocal microscopy measurements. This conclusion can be justified by considering that the examined particles are slightly oval and are likely to have different orientations during the two stages of microscopy and compression testing. For cold spraying of the powder with typical processing conditions, the calculated velocity ratio (v_p/v_{cr}) showed a noticeable variation (around 10%) when the UTS was considered as a function of particle size. The results underline the importance of such compression tests and the associated analysis for characterisation and tailoring of feedstock powder for cold spray applications. Clearly, for a more reliable estimation of the properties in practical cases, the number of examined particles can be more than what has been considered in this study. The new procedure can also be used to investigate correlations between solidification microstructures and the associated particle properties, thus setting grounds for new developments in powder manufacturing and powder metallurgy.

Author Contributions: Conceptualization, H.A.; methodology, H.A. and F.G.; software, H.A.; validation, F.G.; formal analysis, H.A.; investigation, F.G.; resources, F.G.; writing—original draft preparation, H.A.; writing—review and editing, F.G. All authors have read and agreed to the published version of the manuscript.

Funding: This research received no external funding.

Acknowledgments: The authors thank Marion Kollmeier from Helmut-Schmidt-University, Hamburg, Germany for experimental analysis and Thomas Gartner from Lufthansa Technik AG, Hamburg, Germany for supplying the material.

Conflicts of Interest: The authors declare no conflict of interest.

References

1. Dykhuizen, R.C.; Smith, M.F. Gas dynamic principles of cold spray. *J. Therm. Spray Technol.* **1998**, *7*, 205–212. [CrossRef]
2. Papyrin, A.; Kosarev, V.; Klinkov, S.; Alkhimov, A.; Fomin, V.M. *Cold Spray Technology*; Elsevier: Amsterdam, The Netherlands, 2006.
3. Assadi, H.; Kreye, H.; Gärtner, F.; Klassen, T. Cold spraying—A materials perspective. *Acta Mater.* **2016**, *116*, 382–407. [CrossRef]
4. Chandler, H.W.; Sands, C.M.; Song, J.H.; Withers, P.J.; McDonald, S.A. A plasticity model for powder compaction processes incorporating particle deformation and rearrangement. *Int. J. Solids Struct.* **2008**, *45*, 2056–2076. [CrossRef]
5. Assadi, H.; Irkhin, I.; Gutzmann, H.; Gärtner, F.; Schulze, M.; Vidaller, M.V.; Klassen, T. Determination of plastic constitutive properties of microparticles through single particle compression. *Adv. Powder Technol.* **2015**, *26*, 1544–1554. [CrossRef]
6. Pérez-Andrade, L.I.; Gärtner, F.; Villa-Vidaller, M.; Klassen, T.; Muñoz-Saldaña, J.; Alvarado-Orozco, J.M. Optimization of Inconel 718 thick deposits by cold spray processing and annealing. *Surf. Coat. Technol.* **2019**, *378*, 124997. [CrossRef]
7. Assadi, H.; Schmidt, T.; Richter, H.; Kliemann, J.O.; Binder, K.; Gärtner, F.; Kreye, H. On parameter selection in cold spraying. *J. Therm. Spray Technol.* **2011**, *20*, 1161–1176. [CrossRef]
8. Kinetic Spray Solutions. Available online: http://www.kinetic-spray-solutions.com (accessed on 7 May 2020).
9. Mauer, G.; Singh, R.; Rauwald, K.H.; Schrüfer, S.; Wilson, S.; Vaßen, R. Diagnostics of Cold-Sprayed Particle Velocities Approaching Critical Deposition Conditions. *J. Therm. Spray Technol.* **2017**, *26*, 1423–1433. [CrossRef]
10. See e.g. Data on HP Alloy 718, (a) 0% Cold Worked, Not Aged, and (b) 5% Cold Worked, Aged, from High Performance Alloys, Inc. Available online: http://www.matweb.com (accessed on 7 May 2020).
11. Special Metals. *Product Handbook of High-Performance Alloys*; Special Metals: New Hartford, NY, USA, 2012.

12. Bagherifard, S.; Roscioli, G.; Zuccoli, M.V.; Hadi, M.; D'Elia, G.; Demir, A.G.; Guagliano, M. Cold spray deposition of freestanding Inconel samples and comparative analysis with selective laser melting. *J. Therm. Spray Technol.* **2017**, *26*, 1517–1526. [CrossRef]
13. Ma, W.; Xie, Y.; Chen, C.; Fukanuma, H.; Wang, J.; Ren, Z.; Huang, R. Microstructural and mechanical properties of high-performance Inconel 718 alloy by cold spraying. *J. Alloys Compd.* **2019**, *792*, 456–467. [CrossRef]
14. Assadi, H.; Greer, A.L. Site-ordering effects on element partitioning during rapid solidification of alloys. *Nature* **1996**, *383*, 150–152. [CrossRef]
15. Schwarz, M.; Karma, A.; Eckler, K.; Herlach, D.M. Physical mechanism of grain refinement in solidification of undercooled melts. *Phys. Rev. Lett.* **1994**, *73*, 1380. [CrossRef] [PubMed]
16. Li, C.J.; Wang, H.T.; Zhang, Q.; Yang, G.J.; Li, W.Y.; Liao, H.L. Influence of Spray Materials and Their Surface Oxidation on the Critical Velocity in Cold Spraying. *J. Therm. Spray Technol.* **2010**, *19*, 95–101. [CrossRef]
17. Greer, J.R.; Oliver, W.C.; Nix, W.D. Size dependence of mechanical properties of gold at the micron scale in the absence of strain gradient. *Acta Mater.* **2005**, *53*, 1821–1830. [CrossRef]
18. Greer, J.R.; De Hosson, J.T.M. Plasticity in small-sized metallic systems: Intrinsic versus extrinsic size effect. *Prog. Mater. Sci.* **2011**, *56*, 654–724. [CrossRef]